

Resonances of ${}^6\text{He}$ via the ${}^8\text{He}(p,t){}^6\text{He}$ reaction

V. Lapoux^{1*}, X. Mougeot¹, N. Keeley^{1,5}, A. Drouart¹, N. Alamanos¹, F. Auger¹, B. Avez¹, D. Beaumel³, Y. Blumenfeld³, R. Dayras¹, C. Force², L. Gaudefroy⁴, A. Gillibert¹, J. Guillo³, H. Iwasaki^{3,7}, T. Al Kalanee², K. W. Kemper⁹, T. Mermizedakis⁶, W. Mittig^{2,10}, L. Nalpas¹, E. Pollacco¹, A. Pakou⁶, T. Roger², P. Roussel-Chomaz², K. Rusek⁵, J-A. Scarpaci³, C. Simenel¹, I. Strojek⁵, D. Suzuki^{3,7,10} and R. Wolski⁸.

(1) CEA-Saclay DSM/IRFU/SPhN Gif-sur-Yvette, France ; (2) GANIL, France ; (3) CNRS-IN2P3, IPN Orsay, France ; (4) CEA-DAM DIF/DPTA/SPN, Bruyères le Châtel, France ; (5) The A. Soltan Institute for Nuclear Studies, Warsaw, Poland ; (6) University of Ioannina, Greece ; (7) University of Tokyo, Japan ; (8) FLNR-JINR, Dubna, Russia ; (9) University of Florida State, USA. (10) NSCL-MSU, USA.

Abstract

We investigated the low-lying spectroscopy of ${}^6\text{He}$ via the 2-neutron transfer reaction induced by the ${}^8\text{He}$ SPIRAL beam at 15.4 A.MeV on a proton-rich target. The light charged recoil particles produced by the direct reactions were measured using the MUST2 Si-strip telescope array. Two new resonances were observed above the known 2^+ state in ${}^6\text{He}$, and the angular momentum transfer was deduced through the analysis of the angular distributions. Results are discussed in comparison with the recent calculations of various nuclear structure theories which include the coupling to the continuum technique and to the ones which give an understanding of the cluster correlations in the light weakly-bound nuclei.

1 Motivations and experimental probe

New interesting phenomena have been observed close to the neutron drip-line, such as halos or neutron skins, and low-lying resonant states. Progress have been reported in the understanding of these exotic structures, related to the weak binding energies of the neutron-rich light nuclei: they can be explained by the interplay between mean field and shell model configurations with cluster structures [1]. However, the nuclear models disagree for the predictions of the spectroscopy of nuclei far away from the valley of stability, due to the different assumptions on nucleon-nucleon interactions, on few-body and pairing correlations, and to our lack of knowledge on crucial microscopic inputs in the nuclear forces, like the expression of the isospin-dependent terms and of the spin-orbit force. The existence and position of resonant states in the light exotic nuclei may provide crucial information to constrain the models and be used benchmarks to test their validity. For near-drip-line nuclei, like ${}^{6,8}\text{He}$ or ${}^{24}\text{O}$, the theories all predict resonant states in the low-lying excitation energy region (below 12 MeV). The characteristics of these states, position, width, spin and parity, have not been firmly established and sometimes they have not been clearly observed. In this context, the region of the light nuclei for $Z \leq 8$ is particularly attracting:

- the nuclear structure offers a rich variety of phenomena related to weakly-bound structures, alpha-cluster like, extended halo or skin structures [1–4], changes in the shell structure are also observed as compared to the shell ordering in the stable nuclei;
- technically, for the systems with a small number of nucleons $A \leq 12$, it is feasible for the theories including the so-called ab-initio or realistic interactions (with 2- and 3-body terms) to carry out analytical calculations and to obtain accurate results within the Green Function Monte Carlo Method (GFMC) [5]. The No-Core Shell Model (NCSM) calculations can be applied to the light nuclei, including different sets of realistic effective interactions. The model was recently extended to include 3-body interaction for the calculations of the low-lying spectra of the p-shell nuclei [6];

*contact e-mail: vlapoux@cea.fr

- for light nuclei close to the drip-line - which means that their particle thresholds are low- their weak binding features have been triggering important development for the understanding of the continuum coupling effects in this region, for the last few years [7–11].
- experimentally the drip-line can be reached, like in the Helium isotopes for which beams at low energies (less than 16 A.MeV) are available at Ganil, this offers the opportunity to measure direct reactions in a low-energy regime, and to investigate both the low-lying spectroscopy and the spectroscopic factors (SF) [12].

In summary the low-lying spectroscopy in this region is the laboratory to test the interplay between shell and cluster structures, correlations and mean field effects, mixing between continuum and discrete states.

In this study, we want to determine the low-lying states of the neutron-rich weakly-bound ${}^6\text{He}$. It has neutron thresholds located at low energy ($S_n = 1.77$ and $S_{2n} = 0.97$ MeV) and no bound excited state. The first excited state is a 2^+ at 1.8 MeV [13]. ${}^6\text{He}$ is now well known as a halo nucleus [4, 14] and the 2n-halo structure was investigated intensively both theoretically and experimentally but the positions, spin and parities of the resonant states above 1.8 MeV are not determined. On the theoretical side, various calculations indicated that a series of 2_2^+ , 1_1^+ , 0_1^+ states should exist above the 2_1^+ state and below the triton-triton S_{t+t} threshold at 12.3 MeV, but they disagree on the energies of these states. These predictions have triggered a lot of experimental activities during the last 15 years. None was successful to determine precisely the energy and width of such states. The main results were obtained via transfer reactions, which indicated resonances below S_{t+t} and broad resonances above. From the ${}^7\text{Li}({}^6\text{Li}, {}^7\text{Be}){}^6\text{He}$ reaction [15], a 2^+ state was indicated at 5.6 with a $\Gamma = 10.9$ MeV width and structures possibly $(1, 2)^-$ at 14.6 ($\Gamma = 7.4$) MeV, and at 23.3 ($\Gamma = 14.8$) MeV; a broad $\Gamma = 4$ MeV at 4 MeV was reported in Ref. [16], and at 18 MeV ($\Gamma = 7.7$) in Ref. [17]. From the ${}^6\text{Li}(t, {}^3\text{He}){}^6\text{He}$ reaction resonance-like structures were seen at 7.7, 9.9 MeV and at 5 and 15 MeV [18]. Experimentally the (p, p') is usually a good probe to search low-lying resonances. But, due to the huge physical background, no resonance except the 2^+ was indicated from a (p, p') experiment done with a GANIL ${}^6\text{He}$ beam and the particle spectroscopy technique [14]. For the observation of the resonant excited states via direct reactions, what we could call the “state preparation” is important: it means that we need to have an entrance channel providing a good overlap with the final state in the exit channel. From the side-product of a previous experiment E405S [19, 20], the 2n-transfer reaction of the ${}^8\text{He}$ SPIRAL beam on a proton-rich target, a foil of polypropylene $(\text{CH}_2)_n$, was indicated as a good probe to explore the excited states of ${}^6\text{He}$. A follow-up experiment (E525S) was defined and carried out with a set-up devoted to the (p, t) measurement, having a better efficiency and larger angular coverage.

2 Measurement of the direct reactions

2.1 Experimental set-up for the (p, t) reactions to the excited states of ${}^6\text{He}$

The (p, t) reactions were measured at GANIL using the ${}^8\text{He}$ SPIRAL beam at 15.4 A.MeV and the new MUST2 Si-strip telescope array [21]. Two beam tracking detectors CATS were used to reconstruct the incident trajectories. The experimental set-up is presented in Fig. 1. Each MUST2 telescope is composed by a first $300\mu\text{m}$ thick Si-strip stage with an active area of 10 cm^2 and 128 X and Y strips. The measurement of the energy loss, time of flight and position is realized by this Si-strip detector. The second stage can be a 4.5 mm thick-SiLi (not used here) and the last one is a 4 cm thick CsI-crystal detector. Time and energy signals are treated under vacuum by front-end ASIC (Application Specific Integrated circuits) electronics. The light charged particles protons (p), deuterons (d) and tritons (t) produced by the elastic, (p, p') and 1- and 2-neutron transfer reactions are measured and identified in the block of 4 telescopes, in coincidence with the He isotopes focused at forward angles in the 5th MUST2 and in the plastic scintillator. Performances of MUST2 in terms of granularity and resolutions correspond to the state of the art: the resolution in the positions dx, dy, is 0.53 mm, giving an angular resolution of 0.53° at 15 cm from the target; the energy resolution of the Si-strips is 40 keV at 5.5 MeV.

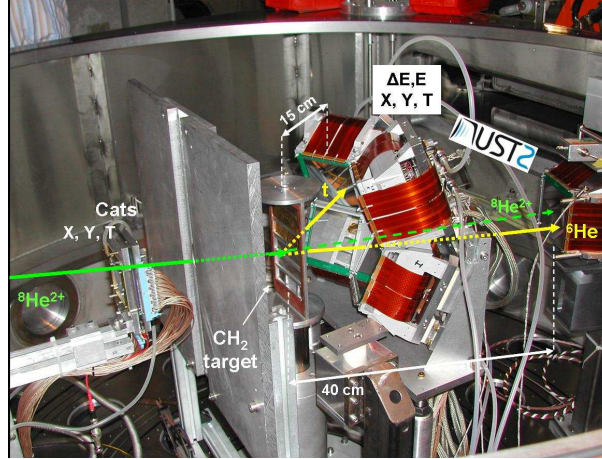


Fig. 1: Experimental set-up including one of the two beam detectors CATS, the array of 4 MUST2 telescope modules located at forward angles at 15 cm from the target, and the 5th telescope used at 0 degrees at 40 cm from the target (it appears rotated in this picture). An additional plastic scintillator (2 cm²) was located at 0 degrees in front of the 5th telescope.

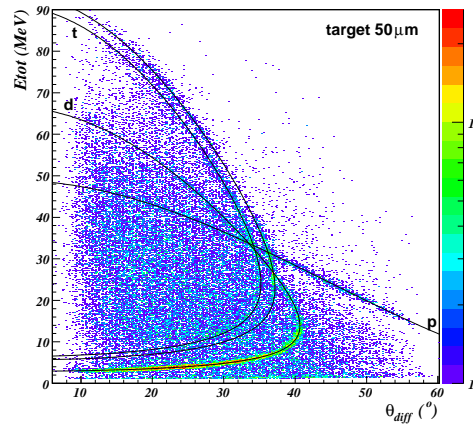


Fig. 2: Kinematics of the measured reactions of ⁸He on proton at 15.4 A.MeV. The lines are the calculated kinematics for the (p,p), (p,d)⁷He_{gs}, and (p,t)⁶He_{gs}, (p,t)⁶He₂₊.

2.2 Kinematics and missing mass method

The results for the direct reactions on the proton target are presented in Fig. 2 for all the events obtained with the 50 μm -thick target (4.48 mg/cm²). From the correlations observed in the spectra of energy versus scattering angle in laboratory (lab.) frame for the tritons, deuterons and protons, and with the kinematical parameters of these particles, the excitation spectra are deduced via the missing mass method for ⁶He, ⁷He and ⁸He, respectively. The particle spectroscopy gives access to both bound excited and resonant states. Here we focus on the ⁶He case and give a summary of the analysis. A complete description will be given in a forthcoming article [22] and the discussion of the spectra for ⁷He via the (p,d) transfer reaction will be developed also in a next article.

3 Analysis of the excitation spectra of ⁶He

The excitation energy spectrum of ⁶He is deduced by missing mass method, from the kinematical characteristics of the triton, the energy and position measured in the MUST2 array, by considering the events with t+⁶He coincidences (corresponding to the ⁶He ground state (gs) in exit channel) and α+t coin-

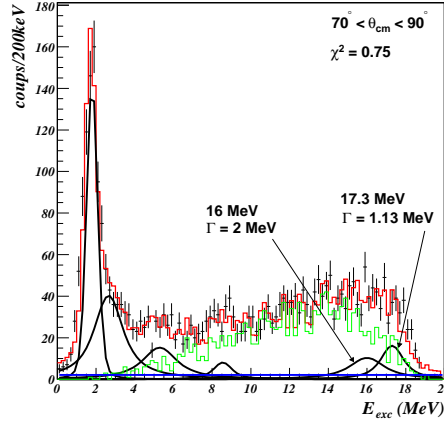


Fig. 3: Example of the analysis for an excitation spectrum of ${}^6\text{He}$ obtained from $\alpha+t$ correlations and for a slice of the kinematics corresponding to the angular range $[70, 90]_{cm}^\circ$. The data with the statistical errors are indicated with the black crosses. The final spectrum (red curve) is obtained by summing the background due to the Carbon (blue line), the phase space (green) and the resonances (black curves).

cidences (which include the events producing unbound excited states of ${}^6\text{He}$). The resolution in the excitation energies for the 4.48 mg/cm^2 thick CH_2 target is of the order of 720 keV.

A structure extracted from the data spectra can be considered as a resonant nuclear state if the parameters (position and width) are conserved within error bars, whatever the angular center of mass (c.m) slice examined between 60 and 150° , the angular range of our experiment. The extraction of resonances was realized in three steps. First the physical background was estimated. The first source is the contribution due to the decay of the exit channel particles ${}^6\text{He}^*$ into $\alpha + n + n$. These many-body kinematical effects are modelled by phase space calculations including the experimental response of the set-up (green curve in Fig. 3). It is interesting to note that at large excitation energies for $E > 14 \text{ MeV}$, the only way to reproduce the shape of the data is to introduce a resonance at 15 MeV . in addition to the the phase space contributions. This resonance is consistent with the data obtained in Ref. [18]. The Carbon content in the target also produces possible reactions with an α in coincidence with a triton. This contribution was estimated from the measured yields on a pure Carbon target, which could be fitted by a simple linear function. The 2^{nd} step was the subtraction of the physical background to find out the possible resonance location. We adopted the Breit-Wigner parametrization to define the distribution of a resonance with the energy E_R and intrinsic width Γ_R :

$$f(E) = \frac{1}{\pi} \frac{\Gamma_R/2}{(E - E_R)^2 + (\Gamma_R/2)^2}, \quad (1)$$

The possible resonances were modelled as Breit-Wigner shapes folded with a Gaussian function, to take into account the experimental spreading due to the experimental resolution. In the search for resonances above the 2_1^+ , the parameters of the peaks corresponding to the gs and 2_1^+ were kept fixed to the known values, which were verified as accurate to reproduce the (p,t) kinematics to the 0_{gs}^+ and to the 2_1^+ . For each angular slices in the c.m frame, the parameters of the resonances (position, width and normalization) were fitted on the subtracted spectra. The number of the possible resonances were also varied to check out the consistency.

Finally, the total excitation spectra (non-subtracted) for ${}^6\text{He}$ were analyzed for different angular slices in the c.m. frame to check the consistency of the extracted parameters of the possible resonances. The search of resonances was done for the various slices $[65;75]$, $[75;85]$, $[85;95]$, $[95;115]$ and $[115;150]^\circ$ c.m. The χ^2 minimization between the data and the calculated curve was considered for

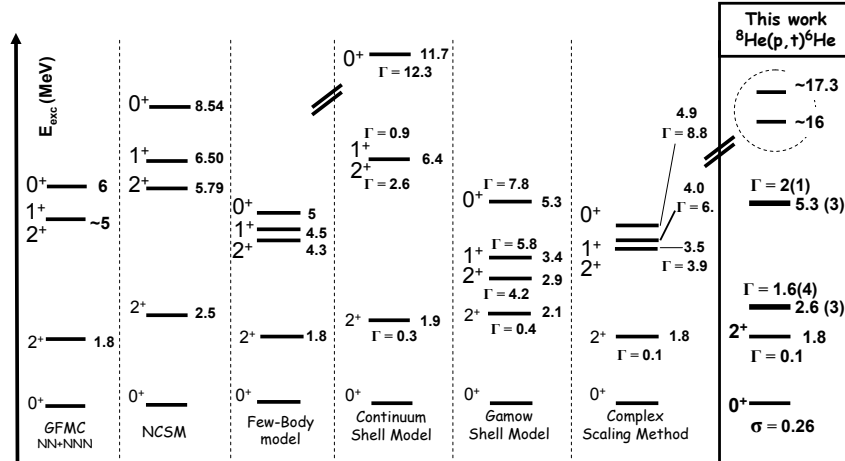


Fig. 4: Spectroscopy of ${}^6\text{He}$: comparison between our new results obtained via ${}^8\text{He}(p,t)$, and several theories, ab-initio GFMC [5], NCSM [24], few-body model [23], CSM [8], GSM [9], and the Complex Scaling Method [10].

the energy range between 0 and 20 MeV, with the 2_1^+ fixed peak, 3 resonances in search, two broad structures located at 16 and 17.3 MeV and adding the total physical background curve. In the search, the normalisation of all the peaks and resonances (even the 2_1^+ one with fixed positions and width) were free to vary. The resulting calculated curve is shown by the red line in Fig. 3. A structure observed around 8 MeV was not considered as a state since it was not observed for all the slices we considered between 60 and 150°c.m. In addition to the known resonance 2_1^+ that we have observed and then fixed in the search at 1.8(2) MeV ($\Gamma = 0.1 \pm 0.2$ MeV) - consistent with the tabulated values (1.8 MeV and 113 keV), two new resonances were found:

at 2.6 ± 0.3 MeV with an intrinsic width $\Gamma = 1.6 \pm 0.4$ MeV and at 5.3 ± 0.3 MeV with $\Gamma = 2 \pm 1$ MeV. Two structures are observed between 15 and 18 MeV. Since they are at the limit of our geometrical efficiency, their positions are not determined precisely from our measurement. However they are consistent with the broad structures observed in previous experiments (see Sec. 1).

3.1 Comparison to the theories

The resonances measured for ${}^6\text{He}$ are compared to the calculations done within various theoretical frameworks: the few-body model [23], the GFMC [5], the NCSM [24], the models treating explicitly the continuum couplings of bound and scattering states [8,9], and recently the Complex Scaling Method [10]. As can be seen in Fig. 4, the best description is given by the models including the continuum couplings, they provide a better treatment of the resonant states, and found them at lower energies than in the other models.

4 Interpretation of the angular distributions, the CRC analysis

The statistical error is included within the points of Figs. 5-6. The systematical errors, including the ones due to the target, the normalization, the efficiency and the subtraction of the background were estimated to the level of 11% (total error bar). Our new data at 15.4 A.MeV are in agreement with the previous data obtained at 15.6 A.MeV [20] and presented in Fig. 5. The previous angular distributions for ${}^8\text{He}(p,t)$ data were analyzed in the framework of the coupled-reaction-channel (CRC) calculations. This method was showed to be powerful to describe consistently elastic and transfer reactions for a whole set of data for exotic nuclei, like ${}^8\text{He}$ [19,20] and ${}^{10,11}\text{Be}$ [25]. The new data obtained at 15.4 A.MeV are consistent with our previous measurements and confirm our interpretation for the gs structure of ${}^8\text{He}$.

The analysis of the ${}^8\text{He}+p$ reactions measured at 15.6 A.MeV [19, 20] offered for the first time the possibility to have a full interpretation of the direct reactions induced by an exotic nucleus in the

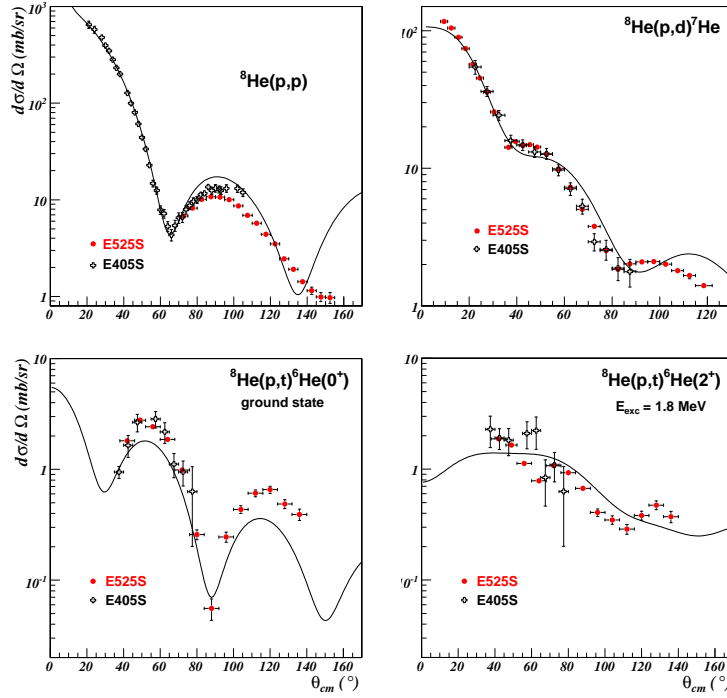


Fig. 5: Experimental cross sections for ${}^8\text{He}(p,p)$, ${}^8\text{He}(p,d){}^7\text{He}_{g.s.}$, ${}^8\text{He}(p,t){}^6\text{He}_{g.s.}$ and $(p,t){}^6\text{He}_{2^+}$. The previous data obtained at 15.6 A.MeV are presented in black dots (“E405S”), the new ones at 15.4 A.MeV are in red (E525S). The curves are CRC calculations at 15.6 A.MeV described in the text.

CRC framework, since the reaction data set included both elastic and $1n$, $2n$ transfer on proton, with a large angular range covered for all the processes. The spectroscopic factors (SF) of the ${}^8\text{He}_{g.s.}$, respected to ${}^7\text{He}_{3/2^-}$ g.s. and ${}^6\text{He}(0^+)$ and ${}^6\text{He}(2^+)$ were deduced [20]: the C^2S values are 2.9, 1.0 and 0.014, respectively. Error bars on the SF are of the order of 30%. These factors are in agreement with the results obtained from the analysis of the quasi-free scattering of ${}^8\text{He}$ measured at GSI [27]: they found the ${}^8\text{He}/{}^6\text{He}_{0^+}$ overlap of 1.3 ± 0.1 ; and the S.F. for ${}^8\text{He}/{}^7\text{He}_{3/2^-}$ was of 3.3 ± 0.3 . The S.F. correspond to a structure for the ${}^8\text{He}$ gs mainly built on the ${}^6\text{He}_{0^+} + 2n$ configuration. The extracted SF indicate a mixing between the $(1p_{3/2})^4_\nu$ and $(1p_{3/2})^2(1p_{1/2})^2_\nu$ neutron configurations in the ${}^8\text{He}$ gs. The consistency with the other existing data was checked. At RIKEN, the (p,t) was measured at 61.3 A.MeV [26]. The SF obtained from our CRC analysis of the (p,t) are in contrast with the ones (both equal to 1) deduced from the DWBA analysis done in Ref. [26]. However, the RIKEN data were reanalyzed successfully within the CRC framework [20] using the same SF inputs as the ones extracted from our SPIRAL data. This study demonstrates how important the reaction framework is to draw correct conclusions on the S.F. and to deduce the microscopic structure. Our results corroborate the configurations found in ${}^8\text{He}_{g.s.}$ by the $\alpha + 4n$ calculations [28]: 34.9% in $(1p_{3/2})^4$; 23.7% in $(1p_{3/2})^2(1p_{1/2})^2$.

The (p,t) cross sections to the new states found in ${}^6\text{He}$ have also been extracted. The transferred angular momentum L_t can be deduced from the analysis of these angular distributions. New calculations taking into account the coupling to these states should be performed in the CRC framework including possible 2-step processes as it was done for the first 2^+ state. However, in Fig. 6, we only present the comparison of the data with a simplified one-step calculations, the aim being to obtain the transferred momentum of the new states. These calculations consider the 0^+ transfer pair of 2 neutrons between the 0^+ gs of ${}^8\text{He}$ and the excited state of ${}^6\text{He}$. The L_t values obtained are 2 and 1 for the two states, respectively. This corresponds to the 2.65 MeV state being a 2^+ . Ambiguity remains for the 5.3 MeV state, it is a 1^- in the simple calculation with a pair transfer but, as we saw for the interpretation of the cross sections to the 2^+_1 , the 2-step process is needed to conclude about the configurations produced by

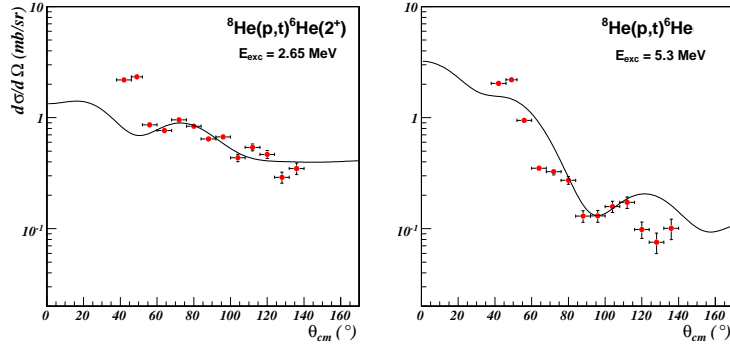


Fig. 6: Angular distributions of the (p,t) reaction to the state at 2.65 MeV (left side) and at 5.3 MeV (right). See the text for the explanation of the spin, parity of these states.

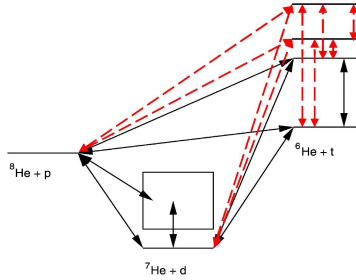


Fig. 7: New CRC scheme required to take into account the coupling to the new resonances found in this work.

the (p,t) reaction. The state at 5.3 MeV could turn out to be a 1^+ , as indicated by the various theories. The figure 7 presents the new CRC scheme proposed for further analysis. The coupling to the channels involving the two new states will be needed. The SF could also be extracted and be compared to the ones provided by the complex scaling method. This will offer the possibility to check how the cluster structures evolve as the excitation energies increase.

5 Conclusions

The results obtained via the $^8\text{He}(p,t)$ reaction are for the moment the most complete ones collected for the low-lying spectroscopy of ^6He , with the evidence of two new resonances and the measurement of a whole set of angular distributions. The new cross sections of ^8He on proton are in agreement with our previous measurements. The interpretation for the ^8He gs, obtained via the CRC analysis [20] are confirmed: the gs includes not only the $(1p_{3/2})^4_\nu$ but also the $(1p_{3/2})^2(1p_{1/2})^2_\nu$ configurations, and this is consistent with the recent dineutron cluster structure discussed by the AMD theory [29].

The new states of ^6He , at 2.6 (3) and at 5.3 (3) MeV were found consistent with a 2^+ and an $L_t = 1$ state respectively. Further analysis is needed to determine the parity of the $L_t = 1$ state. The resonances were compared to the predictions of microscopic models. The agreement is satisfactory with the theoretical predictions in Ref [9, 10]. These approaches include explicitly the continuum-coupling effect to the resonant and scattering states, and provide a good description of the $\alpha + xn$ cluster structures. The important feature of these models is their realistic treatment of the coupling to the continuum: the two neutrons of the halo can interact with each other and be excited to the continuum states. They seem to be promising for the development of accurate spectroscopic descriptions of the exotic nuclei.

The (p,t) transfer reaction induced by ^8He at 15.4 A.MeV was a good probe for the exploration of ^6He resonances. These direct reactions on proton target and the particle spectroscopy technique using the MUST2 array or the next-generation devices will be the adequate tool for a systematic investigation of spectroscopic factors and resonant states of exotic nuclei, specially in the scope of the SPIRAL2

development of beams at low-energy below 20 A.MeV.

Acknowledgements

We wish to thank the SPEG staff P.Gangnant and J-F. Libin and the Ganil GIP group for their help in the setting of the experiment.

References

- [1] Contributions to this conference *Varenna09*, talks and references during the Ikeda session; K . Ikeda, H. Horiuchi, Y. Kanada-En'yo, H. Masui, T. Myo.
- [2] I. Tanihata *et al.*, Phys. Rev. Lett. **55**, 2676 (1985); Phys. Lett. **B289**, 261 (1992).
- [3] M. V. Zhukov *et al.*, Phys. Rep. **231**, 151 (1993).
- [4] B. Jonson, Phys. Rep. **389**, 1 (2004).
- [5] S.C. Pieper, R.B. Wiringa, and J. Carlson, Phys. Rev. C **70**, 054325 (2004). S.C. Pieper *et al.*, Nucl. Phys. **A751**, 516c (2005).
- [6] P. Navrátil and W. E. Ormand, Phys. Rev. C **68**, 034305 (2003).
- [7] N. Michel, W. Nazarewicz, M. Ploszajczak and K. Bennaceur, Phys. Rev. Lett **89**, 042502 (2002); N. Michel, W. Nazarewicz, M. Ploszajczak and J. Okolowicz, Phys. Rev. C **70**, 054325 (2004).
- [8] A. Volya and V. Zelevinsky, Phys. Rev. Lett. **94**, 052501 (2005).
- [9] G. Hagen, M. Hjorth-Jensen, J.S. Vaagen, Phys. Rev. C **71**, 044314 (2005).
- [10] T. Myo, K. Kato, K. Ikeda, Phys. Rev. C **76**, 054309 (2007).
- [11] H. Masui, K. Kato, and K. Ikeda, Phys. Rev. C **75**, 034316 (2007).
- [12] F. Skaza *et al.*, Nucl. Phys. **A788** (2007) 260c.
- [13] D.R. Tilley *et al.*, *Energy levels of light nuclei A = 5, 6, 7*, Nucl. Phys. **A708**, 3 (2002).
- [14] A. Lagoyannis *et al.*, Phys. Lett. B **518**, 27 (2001).
- [15] J. Jänecke *et al.*, Phys. Rev. C **54**, 1070 (1996).
- [16] S. Nakayama *et al.*, Phys. Rev. Lett. **85**, 262 (2000).
- [17] H. Akimune *et al.*, Phys. Rev. C **67**, 051302 (2003).
- [18] T. Nakamura *et al.*, Phys Lett B **493**, 209 (2000) ; Eur. Phys. J. A **13**, 33 (2002).
- [19] F. Skaza *et al.* Phys. Lett. B **619**, 82 (2005); Phys. Rev. C **73**, 044301 (2006).
- [20] N. Keeley *et al.*, Phys. Lett B **646**, 222 (2007).
- [21] E. Pollacco *et al.*, Eur. Phys. J. A **25**, 287 (2005).
- [22] X Mougeot, V. Lapoux *et al.*, *New resonant states of ${}^6\text{He}$ via ${}^8\text{He}(p,t)$ reaction*, to be submitted.
- [23] B.V. Danilin *et al.*, Phys. Rev C **55**, 577 (1997).
- [24] P. Navrátil and B.R. Barrett, Phys. Rev. C **57**, 3119 (1998); and P. Navrátil, private co.
- [25] N. Keeley and V. Lapoux, Phys. Rev C **77**, 014605 (2008).
- [26] A.A. Korshennikov *et al.*, Phys. Rev. Lett. **90**, 082501 (2003).
- [27] L.V. Chulkov *et al.*, Nucl. Phys. **A759**, 43 (2005).
- [28] K. Hagino, N. Takahashi, H. Sagawa, Phys. Rev. C **77**, 054317 (2008).
- [29] Y. Kanada-En'yo, Phys. Rev. C **76**, 044323 (2007).